

RF MEMS Capacitive Switches for Integration with Printed Circuits and Antennas

R. Ramadoss¹, S. Lee², V. M. Bright², Y. C. Lee², and K. C. Gupta¹

¹Department of Electrical and Computer Engineering, ²Department of Mechanical Engineering
University of Colorado at Boulder, Boulder, CO 80309-0425, USA

Abstract — RF MEMS capacitive switches fabricated using flexible printed circuit technology have been reported by our group recently. In this paper, we report new switch designs for X/Ku band operation and their mechanical and RF performance. For operation in X/Ku-band frequency ranges, the switch plate dimensions have been reduced to $2 \times 1 \text{ mm}^2$, which is a reduction of our earlier switch design $6 \times 6 \text{ mm}^2$ by a factor of 18. This remarkable reduction in size necessitated significant improvements in the switch design. Specific improvements such as low pull-down voltage design, membrane warpage reduction, and improved RF design are discussed. Resistive bias arrangement for this type of switches is discussed. Pull-down voltage of these switch designs is in the range of 80-100 Volts. RF performance with insertion loss $< 0.3 \text{ dB}$ and isolation $> 10 \text{ dB}$ has been demonstrated in the frequency range of 8 to 20 GHz.

I. INTRODUCTION

In recent years, there has been considerable interest in the development of Microelectromechanical system (MEMS) fabricated using traditional printed circuit board (PCB) materials and processing techniques. The dimensions of PCB based MEMS components are of the order of mils. MEMS components such as micropumps, microchannels, flow sensors and salinity sensors have been developed using the PCB technology (For example see [1]). The unique advantages of PCB based MEMS include low cost, high volume fabrication, and integration with printed circuit components. Further, use of PCB processing enables ease of integration of MEMS devices with associated control electronics and fabrication of complex multi-layer 3D structures.

RF MEMS switches have proved to exhibit better performance compared to semiconductor based switching circuits [2]. Recently, our group demonstrated a new type of electrostatically actuated RF MEMS capacitive switches using flexible printed circuit technology [3]. These switches are uniquely suitable for batch integration with printed circuit board (PCB) based RF circuits and antennas. In this paper, we report mechanical design, RF design, and performance of flexible printed circuit based X/Ku-band capacitive switches.

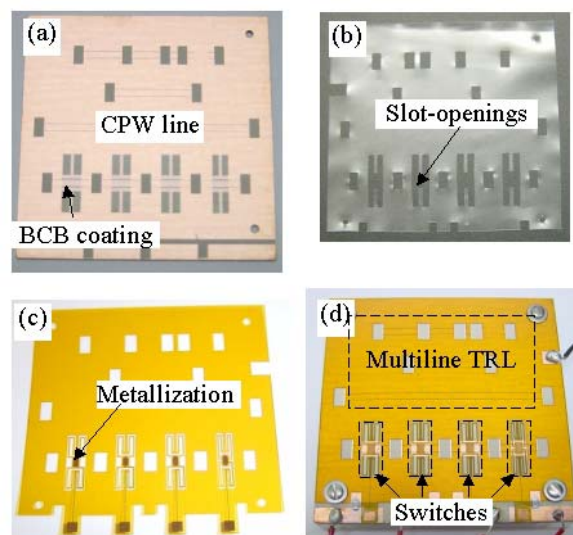


Fig. 1. Photographs of (a) CPW line with BCB dielectric layer on duroid substrate (b) adhesive spacer film with milled slot-openings (c) Kapton E polyimide film with switch top electrode metallization and laser machined slot-openings (d) assembled switch prototype.

II. FABRICATION AND ASSEMBLY

The switch consists of three layers: substrate, adhesive spacer film, and polyimide film. Photographs of different layers and assembled prototype of X/Ku band switches are shown in Fig. 1(a)-(b). CPW lines for mounting switches and multi-line TRL calibration lines are defined on the metallization layer of duroid substrate. Photosensitive benzocyclobutene (BCB) dielectric layer is spin-coated and patterned on CPW lines. Adhesive spacer film is milled to create slot-openings. The switch electrode metallization is patterned on Kapton-E polyimide film, which is machined using excimer laser to create slot-openings. These layers are aligned (using a fixture) and assembled using a thermo-compression bonding cycle. Details of fabrication and assembly of this type of switches are discussed in [3].

III. MECHANICAL DESIGN AND TESTING

A. Mechanical Design Improvements

The switch pull-down voltage (derived considering a one-dimensional spring-capacitor model) is given by

$$V_p = \sqrt{\frac{8kz_o^3}{27A\epsilon_o}} \dots \dots \dots (1)$$

where k is the spring constant of the flexures, A is the area of the plate, z_o is the initial gap height between the plates, and ϵ_o is the permittivity of air.

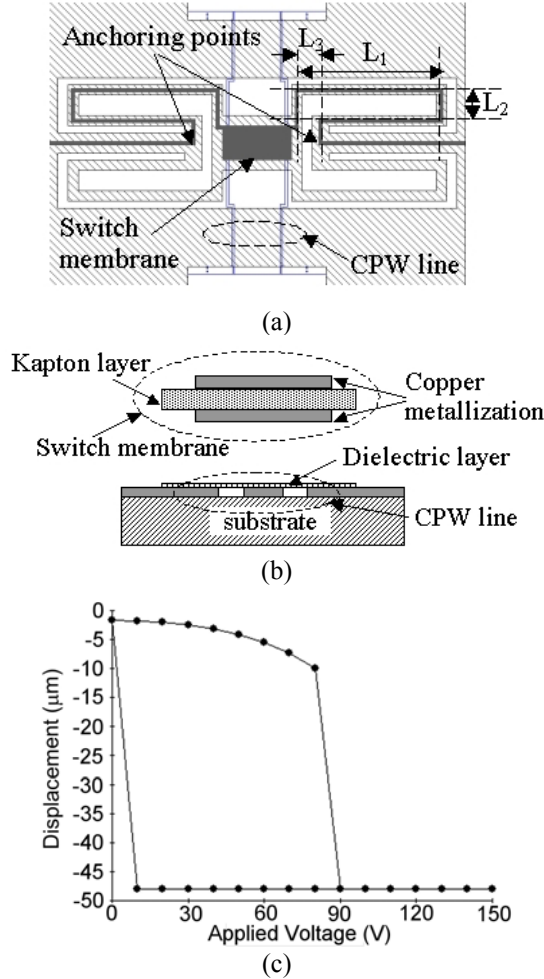


Fig. 2. Mechanical flexure design: (a) top view of flexure design (b) cross section (not to scale) showing identical copper metallization patterns on kapton layer (b) gap-height versus applied voltage characteristics.

For operation in X/Ku-band frequency ranges, the switch plate dimensions have been reduced to $2 \times 1 \text{ mm}^2$, which is a reduction of earlier switch design $6 \times 6 \text{ mm}^2$ reported in [3] by a factor of 18. From Eq. (1), it can be seen that this decrease in area would significantly increase the pull-down voltage due to inverse dependence of V_p on

\sqrt{A} . This remarkable reduction in the switch plate area has been compensated by designing a compliant flexure to provide low pull-down voltage in the range of 60-100 V.

One of the compliant flexure configurations investigated for the design of low pull-down voltage switches is shown in Fig. 2(a). This figure shows switch top view with Kapton polyimide film (hatched region), top electrode metallization (solid region), and CPW line metallization. This flexure configuration aids in the reduction of switch membrane warpage and the details are discussed in the next section.

B. Membrane Warpage Reduction

In the assembly process, the switch prototype is heated to 130°C for thermo-compression bonding and cooled down to room temperature [3]. Various layers of the switch (substrate, copper, adhesive spacer film, and kapton polyimide film) have different coefficients of thermal expansion CTE values (16 ppm, 17 ppm, 105 ppm, and 12 ppm, respectively). During the bonding cycle, these layers expand and contract unequally due to the mismatch in the CTE values, which causes the warpage of the switch membrane.

Mechanical-thermal simulations (using *MemMech* in [4]) have been carried out to study the switch membrane warpage caused by thermal mismatches between various switch layers. To study the dominant factor that contributes to the overall thermal mismatch three different simulations have been carried out: (a) a model with the kapton layer and the copper metallization only, (b) a model with the kapton layer and the duroid substrate only, and (c) the complete model with all the layers.

Table 1. Mechanical-thermal simulation results for membrane warpage (Positive and negative numbers represent warpage in up and down directions, respectively, with reference to no warpage position).

Case (a): Kapton-copper metallization	+ 30 μm
Case (b): Kapton-duroid	- 7 μm
Case (c): Complete model	+ 22 μm
Case (d): Complete model with two sided copper metallization on Kapton	- 7 μm

From these simulation results (summarized in Table 1), it can be observed that the critical factor that contributes to the membrane warpage is the mismatch between the kapton layer and copper metallization on this layer. To reduce this warpage, switches have been designed and simulated with identical metallization patterns on the two sides of the kapton layer (as shown in Fig. 2(b)). The simulation results (also shown in Table 1) for this design show a significant reduction in the

membrane warpage. This design has been fabricated and the experimental results are discussed in the following sections.

C. Simulation and Experimental results

Switch pull-down voltage is obtained from *CoSolve* simulation (a coupled electromechanical solver available in [4]) that yields switch membrane displacement versus applied voltage characteristics. The flexure dimensions of an example design (that provides low pull-down voltage and possess enough stiffness to restore back to its original position) are $L_1 = 4.2$ mm, $L_2 = 0.9$ mm, $L_3 = 0.7$ mm, and flexure width = 0.3 mm. A number of switches were fabricated and tested. The measured pull-down voltage of these switches is in the range of 80 to 100 Volts. Simulation and experimental results for the gap height in up position and the pull-down voltage are summarized in Table 2. It can be noted that the experimental results show a close agreement with the simulation results.

Table 2. Simulation and Experimental results for an example switch design (shown in Fig. 2)

	Simulated	Measured
Gap height	40 μ m	43-46 μ m
Pull-down Voltage	85 V	80-100 V

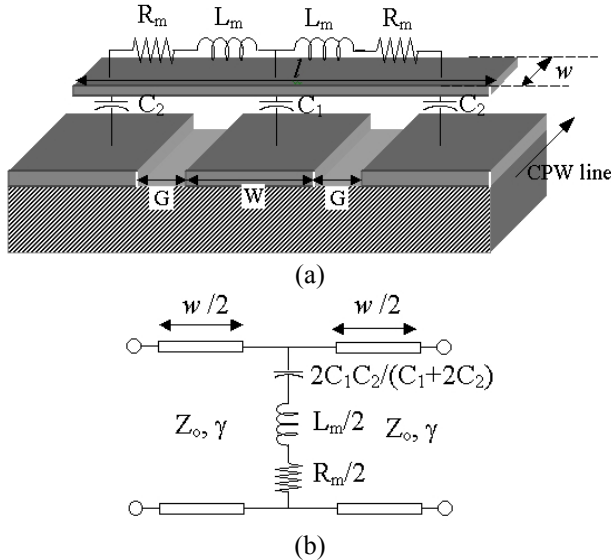


Fig. 3. CPW shunt switch: (a) physical configuration (b) equivalent circuit model

IV. RF DESIGN AND TESTING

A. RF Configuration and Design

Physical configuration and equivalent circuit model of a shunt switch mounted on coplanar waveguide (CPW) are shown in Fig. 3. In this configuration, the total shunt capacitance across the transmission line is given by $C_T = 2C_1C_2/(C_1+2C_2)$. The dimensions of the CPW line are chosen such that the capacitance $C_1 \gg 2C_2$. Consequently, the total capacitances in the up and down positions are given by $C_u \sim 2C_{2u}$ and $C_d \sim 2C_{2d}$, respectively. Thus, the RF capacitances and hence the RF performances of the switch depend mainly on C_{2u} and C_{2d} values. On the other hand, the switch pull-down voltage is related to the DC capacitance (in the biasing circuit) given by $C_{1u}+2C_{2u}$. Thus, this configuration provides flexibility for the design of low pull down voltage ($C_{1u}+2C_{2u}$ can be high) switches with a high self-actuation voltage (which depends on C_{2u}).

The length l and width w of the switch plate are 2 mm and 1 mm, respectively. The dimensions of the CPW line are $W = 1300$ μ m and $G = 250$ μ m. The up-position air gap height is 46 μ m. BCB dielectric layer ($\epsilon_r = 2.65$) of thickness 1 μ m is used. Mechanical flexure configuration (design example discussed in III-C) shown in Fig. 2(a) has been used.

B. Resistive Bias Arrangement

An ideal biasing network should not affect the RF performance of the switch. For broadband biasing of switches, resistive bias arrangement shown in Fig. 4(a) is used. The effect of the bias line resistance on the switch insertion loss has been studied using circuit simulation in [5] and the results are shown in Fig. 4(b). These results show that bias lines with low resistance values exhibit transmission line effects with a significant leakage loss. Further, it can be noted that a resistive bias connection with a total resistance $R_B > 5$ K Ω does not significantly affect the switch RF performance (in ON and OFF states) in the frequency range of 1 to 30 GHz.

In this work, thin film type resistive lines are used for biasing of the switches. The chromium seed layer of 200 Angstroms thick present between the copper layer and the kapton layer is patterned to form resistive bias lines. A test circuit with chromium lines of 55 μ m, 40 μ m, and 25 μ m wide has been fabricated and the resistances of these lines were measured to be 1.4 K Ω /mm, 2.2 K Ω /mm, and 6.5 K Ω /mm, respectively. Resistive bias lines of 25 μ m wide and 2 to 4 mm long that provide a total resistance of $R_B > 10$ K Ω have been used for X/Ku-band switches and the results are discussed in the next section.

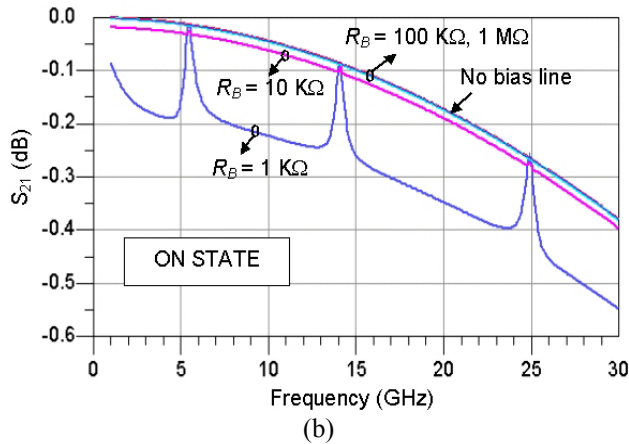
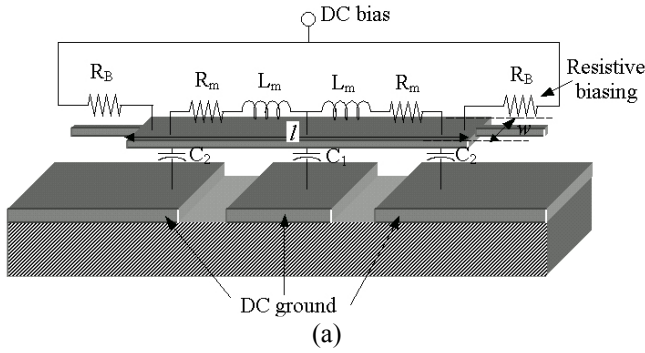


Fig. 4. Resistive bias arrangement: (a) physical configuration (b) effect of bias line resistance on insertion loss

C. Experimental Results

Photograph of a typical switch is shown in Fig. 5(a). Air coplanar probes (ACP40-GSG, Cascade Microtech) of 900 μm pitch have been used for measurements. S-parameter measurements have been carried using multiline TRL calibration of vector network analyzer. The measured insertion loss and isolation of the switch in ON and OFF states, respectively, are shown in Fig. 5(b). Insertion loss is less than 0.3 dB in the frequency range of 6-20 GHz. Isolation is about 10 dB at 8 GHz and 26 dB at 20 GHz. This switch design is suitable for operation in X/Ku-band frequency ranges.

V. CONCLUSION

In this paper, mechanical and RF design of flexible circuit based RF MEMS capacitive switches for X/Ku-band operation are discussed. These switches exhibit pull-down voltage of 80–100 V, insertion loss < 0.3 dB and isolation > 10 dB in the frequency range of 8 to 20 GHz. These switches are uniquely suitable for integration with printed circuits and antennas for reconfigurable applications.

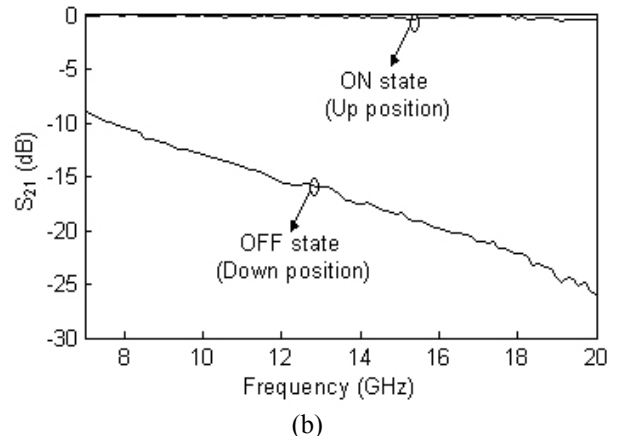
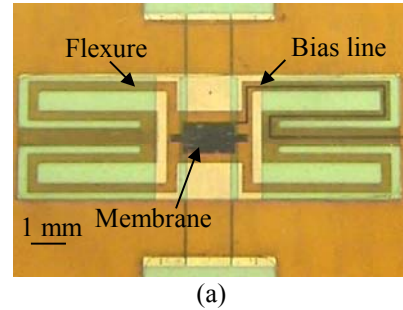


Fig. 5. X/Ku-band switch: (a) photograph (b) measured RF performance

ACKNOWLEDGEMENT

This project has been sponsored by the DARPA RECAP program. The authors would like to acknowledge Dr. P. Watson, AFRL, OH, USA. The authors are grateful to Dr. J. A. Jargon and Dr. D. C. DeGroot at NIST, Boulder, for their help with RF measurements.

REFERENCES

- [1] "Session III: PCB and Polymer For MEMS and Microsystems Packaging," at *Int. Microelectr. Packaging Society (IMAPS) Workshop on Packaging of MEMS and Related Micro Integrated/Nano Systems*, September 6-8, 2002, Denver, Colorado.
- [2] G. M. Rebeiz and J. B. Muldavin, "RF MEMS Switches and Switch Circuits," *IEEE Microwave Magazine*, Dec. 2001, pp. 59-71.
- [3] R. Ramadoss, S. Lee, V. M. Bright, Y. C. Lee, and K. C. Gupta, "Polyimide film based RF MEMS capacitive switches," *IEEE MTT-S Int. Microwave Symp. Dig.*, Seattle, WA, June 2-7, 2002, pp. 1233-1236.
- [4] CoventorWare ver. 2001.3, Coventor Inc., NC, USA.
- [5] Advanced Design System 2001, Agilent Technologies, CA, USA.